Int. J. Electrochem. Sci., 8 **(2013)** 2606 - 2624

International Journal of
ELECTROCHEMICAL
SCIENCE
www.electrochemsci.org

Ionic Conductivity and Transporting Properties in LiTFSI-Doped Bis(trifluoromethanesulfonyl)imide-Based Ionic Liquid Electrolyte

Tzi-Yi Wu[*], *Lin Hao, Pin-Rong Chen, Jian-Wei Liao*

Department of Chemical and Materials Engineering, National Yunlin University of Science and Technology, Yunlin 64002, Taiwan, ROC
[*]E-mail: wuty@yuntech.edu.tw

Received: 24 November 2012 / *Accepted:* 23 January 2013 / *Published:* 1 February 2013

In this research, various molar percents of lithium bis(trifluoromethanesulfonyl)imide (LiTFSI) are incorporated into 1-methyl-3-pentylimidazolium bis(trifluoromethanesulfonyl)imide ([MPI][TFSI]) electrolyte system. The solubility of lithium salt in [MPI][TFSI] is examined, homogeneous binary ILs were obtainable over a wide range of salt concentrations (x_{LiTFSI} = 0 ~ 0.45). Ionic conductivity and transporting properties in mixtures of [MPI][TFSI] and LiTFSI are characterized using a conductivity meter and pulsed field gradient NMR measurements at various temperatures. Temperature-dependent viscosity, ionic conductivity, molar conductivity, and self diffusion coefficient in neat [MPI][TFSI] and LiTFSI-doped [MPI][TFSI] followed the Vogel–Tamman–Fulcher equation at all concentrations. The ionic conductivity and the self-diffusion coefficient of each ionic specie decrease with increasing concentration of LiTFSI in LiTFSI-doped [MPI][TFSI], whereas the lithium transference number increases with increasing concentration of LiTFSI in LiTFSI-doped [MPI][TFSI]. The LiTFSI-doped ILs have many desirable properties for lithium-conducting electrolytes, including high ionicity, a high lithium transference number, in addition to the common properties of ionic liquids, and will thus open a new field of research on ionic liquids.

Keywords: Ionic liquid electrolyte, ionic conductivity, lithium bis(trifluoromethanesulfonyl)imide, Walden's rule, self-diffusion coefficient, lithium ion transference number

1. INTRODUCTION

Ionic liquids (ILs) are salts that are liquids at temperatures below 373.15 K and are composed entirely of ions. They have received considerable attention as alternatives to traditional organic solvents [1-12]. Their intrinsic properties, like negligible vapor pressure, low melting point [13], a wide liquid range, suitable viscosity [14], unique permittivity, high thermal stability, good solvents for

both polar and nonpolar organic and inorganic substances, high electrical conductivity, and wide electrochemical window [15,16], they have been widely used, make them very attractive candidates as electrolytes in rechargeable lithium batteries [17-20], electrochemical sensor [21-37], solar cells [38-43], and fuel cell [44].

Typical ionic liquids, which have been reported, consist of quarternized ammonium cations and anions with low Lewis basicities. Currently, most studies on ILs are dealing with imidazolium derivatives due to low viscosity and good ionic conductivity. If intended to be used in Li batteries, ILs are required to have the ability to dissolve a Li salt to have a high Li^+ conductivity. Accordingly, the fundamental knowledge on conductivity and ionic diffusion properties in LiTFSI-doped bis(trifluoromethanesulfonyl)imide-based ionic liquid electrolyte is important. The translational (or self-) diffusion coefficient (*D*) of a liquid is one of the most important physical parameters for probing solution interactions, and thus additional information is gained by measuring *D* over a temperature range. Pulsed gradient spin echo (PGSE) NMR, coupled with various data processing schemes, is a powerful method for the mixture analysis of *D* owing to (PGSE) NMR method can easily be applied to measure variable temperature diffusion data simply by changing the temperature of the surrounding the sample tube.

In the present work, the impact of the addition of lithium salt on viscosity, conductivity, and ionic dissociation in lithium bis(trifluoromethanesulfonyl)imide (LiTFSI)-doped bis(trifluoromethanesulfonyl)imide-based ionic liquid ([MPI][TFSI]) electrolyte is evaluated. To evaluate the possibility of using binary [MPI][TFSI] and LiTFSI electrolytes, the solubility of lithium salt in [MPI][TFSI] is examined, homogeneous binary ILs were obtainable over a wide range of salt concentrations ($x_{\mathrm{LiTFSI}} = 0 \sim 0.45$). The relationship between the ionic conductivity and the viscosity in the neat [MPI][TFSI] and LiTFSI-doped [MPI][TFSI] is analyzed using the Walden rule. The temperature dependence of the diffusion of the individual species (i.e., anion and cation) in an electrolyte formed by doping [MPI][TFSI] with the lithium salt LiTFSI as a function of the LiTFSI mole fraction *x* were measured using ^1H, ^7Li, or ^{19}F PGSE-NMR, respectively.

2. EXPERIMENTAL

2.1. Materials and measurement

1-Methylimidazole (99%), 1-bromopentane (99%), and lithium bis(trifluoromethanesulfonyl)imide (99%) were obtained from Aldrich, TCI, and Acros and used as received. The conductivity (σ) of the ionic liquid was systematically measured with a conductivity meter LF 340 and a standard conductivity cell TetraCon 325 (Wissenschaftlich-Technische Werkstätten GmbH, Germany). The cell constant was determined by calibration after each sample measurement using an aqueous 0.01 M KCl solution. The density of the ILs was measured with a dilatometer, which was calibrated by measuring the density of neat glycerin at 30, 40, 50, 60, 70, and 80 ^oC. The dilatometer was placed in a thermostatic water bath (TV-4000, TAMSON) whose temperature was regulated to within ± 0.01 K. To measure density, IL or a binary mixture was placed

into the dilatometer up to the mark, the top of the capillary tube (located on the top of the dilatometer) was sealed, and the dilatometer (with capillary tube) was placed into a temperature bath for 10 min to allow the temperature to equilibrate. The main interval between the two marks in the capillary tube was 0.01 cm^3, and the minor interval between two marks was 0.001 cm^3. From the correction coefficient of glycerin in capillary tube at various temperatures, we can calculate the density of neat IL or binary system by the expanded volume of liquid in the capillary tube at various temperatures. Each sample was measured at least three times to determine an average value, and the values of the density were ±0.0001 g/mL. The viscosities (η) of the ILs were measured using a calibrated modified Ostwald viscometer (Cannon-Fenske glass capillary viscometers, CFRU, 9721-A50) with inner diameters of 1.2 ± 2% mm [45-48]. The viscometer was placed in a thermostatic water bath (TV-4000, TAMSON), in which the temperature was regulated to within ± 0.01 K. The flow time was measured with a stop watch capable of recording to 0.01 s. For each IL, the experimental viscosity was obtained by averaging three to five flow time measurements. The water content of the dried ILs was detected by a Karl–Fischer moisture titrator (Metrohm 73KF coulometer), and the values were less than 100 ppm. NMR spectra of synthetized ILs were recorded on a BRUKER AV300 spectrometer and calibrated with tetramethylsilane (TMS) as the internal reference.

2.2. Synthesis of 1-methyl-3-pentylimidazolium bis(trifluoromethanesulfonyl)imide [MPI][TFSI]

1-Bromopentane (208 g, 1.38 mol) was added to a vigorously stirred solution of 1-methylimidazole (102.6 g, 1.25 mol) in toluene (125 mL) at 0 ^oC. The solution was heated to reflux at around 110 ^oC for 24 hours, and then cooled to room temperature for 12 hours. The toluene was decanted and the remaining viscous oil was washed with ether several times to yield a viscous liquid, which was dried *in vacuo* to give 1-pentyl-3-methylimidazolium bromide ([MPI][Br]) with a yield of approximately 82 %. ^{1}H-NMR (400MHz, D_2O, ppm): δ 0.80 (t, J = 7.1 Hz, 3H, CH_3), δ 1.14-1.33 (m, 4H, CH_2), δ 1.76-1.86 (m, 2H, CH_2), δ 3.84 (s, 3H, CH_3), δ 4.14 (t, J = 7.1 Hz, 2H, CH_2), δ 7.37-7.40 (m, 1H, CH), δ 7.42-7.44 (m, 1H, CH), δ 8.67 (s, 1H, CH). Elemental analysis (%) is found (C, 46.26; H, 7.32; N, 11.97) and calculated (C, 46.36; H, 7.35; N, 12.02) for synthetic [MPI][Br]. An aqueous solution of lithium bis(trifluoromethylsulfonyl)imide (100 mmol, 28.7 g) was then added to an aqueous solution of [MPI][Br] (100 mmol, 23.3 g). The mixture was reacted for 3 h at 60 ^oC. After cooling, a white oily product was formed, which was extracted with chloroform. After removing the solvent under reduced pressure, a colorless oily product was obtained. Then, the combined solution was dried in a vacuum at 100 ^oC to remove the water. Yield: 91%. ^{1}H NMR (300 MHz, DMSO-d_6, ppm): 8.99 (s, 1H, hydrogen of imidazolium), 7.64 (d, 1H, hydrogen of imidazolium), 7.57 (d, 1H, hydrogen of imidazolium), 4.05 (t, 2H, N–CH_2–), 3.75 (s, 3H, N–CH_3), 1.69 (m, 2H, N–CH_2–CH_2–), 1.22 (m, 2H, N–CH_2–CH_2–CH_2–), 1.13 (m, 2H, N–CH_2–CH_2–CH_2–CH_2–), 0.77 (t, 3H, N–CH_2–CH_2–CH_2–CH_2–CH_3). ^{19}F NMR(400 MHz, DMSO-d_6): 82.8 ppm. Elem. Anal. Calcd. for $C_{11}H_{17}F_6N_3O_4S_2$: C, 30.48%; H, 3.95%; N, 9.70%. Found: C, 30.35%; H, 3.91%; N, 9.58%. The Br^- contents were confirmed with ICP-MS, which was below 0.5% w/w.

2.3. Sample preparation for diffusion coefficient measurements

A portion of each sample was degassed and sealed in a cylindrical Pyrex tube under high vacuum at room temperature. The sealed sample tube was inserted into a standard 5 mm tube filled with an external lock solvent of D_2O. ^1H, ^{19}F, ^7Li NMR measurements were carried out on a Bruker Avance 400 with a 5 mm pulsed-field gradient probe. The signals of ^1H in $[MPI]^+$, ^7Li in Li^+, and ^{19}F in bis(trifluoromethanesulfonyl)imide anion were used for the determination of self-diffusion coefficients (D_{MPI^+} , D_{Li^+} , and D_{TFSI^-}) of the cation and anion species, respectively. The sample temperature was controlled within ±0.1K by a variable temperature control unit using heated.

Pulsed-gradient spin-echo diffusion measurements were carried out using a stimulated spin-echo sequence. In the pulsed-field gradient spin-echo NMR experiment, the self-diffusion coefficient, *D*, is given by Tanner and Stejskal [49]:

$$\ln\left(\frac{A}{A_0}\right) = -D\gamma^2(\Delta - \frac{\delta}{3})\delta^2 g^2 \qquad (1)$$

where A and A_0 are the signal integrals in the presence and absence of the pulsed-field gradient, respectively, γ is the nuclear magnetogyric ratio, Δ is the interval between the two gradient pulses, δ is the gradient pulse width, and g is the gradient magnitude. In the present experiments, the pulse-field-gradient interval Δ determines the diffusion time and was varied from 20 to 100 ms, δ was set between 3 and 18 ms, and g was set using a suitable strength. The self-diffusion coefficients were measured five or more times at each temperature. The experimental errors in D_{MPI^+} , D_{Li^+} , and D_{TFSI^-} were estimated to be less than 3%.

3. RESULTS AND DISCUSSION

3.1. Ionic conductivity and viscosity of neat [MPI][TFSI] and LiTFSI-doped [MPI][TFSI]

The fundamental properties of neat [MPI][TFSI] and LiTFSI-doped [MPI][TFSI], including physicochemical quantities of density (ρ), viscosity (η), and conductivity (σ), are plotted in Fig. 1-3, all of the LiTFSI-doped [MPI][TFSI] are liquid at room temperature.

Generally, in a narrow range of temperatures, ρ (g cm^{-3}) can be expressed as follows:

$$\rho = a + bT \qquad (2)$$

where a, b, and T are the density at 0 K (g cm^{-3}), the coefficient of volume expansion (g cm^{-3} K^{-1}), and temperature (K), respectively. In the present system a strong linear relationship ($r > 0.999$) with temperature was obtained for neat [MPI][TFSI] and LiTFSI-doped [MPI][TFSI] (Fig. 1). The best fit parameters of Eq. (2) are summarized in Table 1. As shown in Fig. 1, the density of lithium bis(trifluoromethanesulfonyl)imide-doped RTIL increases with increasing lithium bis(trifluoromethanesulfonyl)imide concentration, for instance, LiTFSI-doped [MPI][TFSI] (x_{LiTFSI} =

0.2516, ρ = 1.4899 g cm^{-3} at 30 ^{o}C) has higher density than IL without doping LiTFSI (ρ = 1.4056 g cm^{-3} at 30 ^{o}C), x_{LiTFSI} = 0.3502 (ρ = 1.5287 g cm^{-3} at 30 ^{o}C) has higher density than x_{LiTFSI} = 0.3006 (ρ = 1.5073 g cm^{-3} at 30 ^{o}C). In lithium bis(trifluoromethanesulfonyl)imide-doped RTIL, a more efficient packing and/or attractive interaction occurred when the ionic liquid and LiTFSI were mixed, small lithium ion fit into the interstices upon mixing. Therefore, the filling effect of lithium ion in the interstices of ionic liquids contributes to a denser structure.

Table 1. The adjustable parameters of density ($\rho = a + b \cdot T$) for neat [MPI][TFSI] and LiTFSI-doped [MPI][TFSI] at various LiTFSI concentrations.

Mole fraction of LiTFSI	ρ		
	a	$10^4 b$	R^{2a}
neat [MPI][TFSI]	1.665	–8.556	0.9999
x_{LiTFSI} = 0.2516	1.770	–9.239	0.9998
x_{LiTFSI} = 0.3006	1.796	–9.523	0.9997
x_{LiTFSI} = 0.3502	1.821	–9.643	0.9998
x_{LiTFSI} = 0.4015	1.836	–9.798	0.9999
x_{LiTFSI} = 0.4502	1.873	–9.995	0.9998

[a] Correlation coefficient.

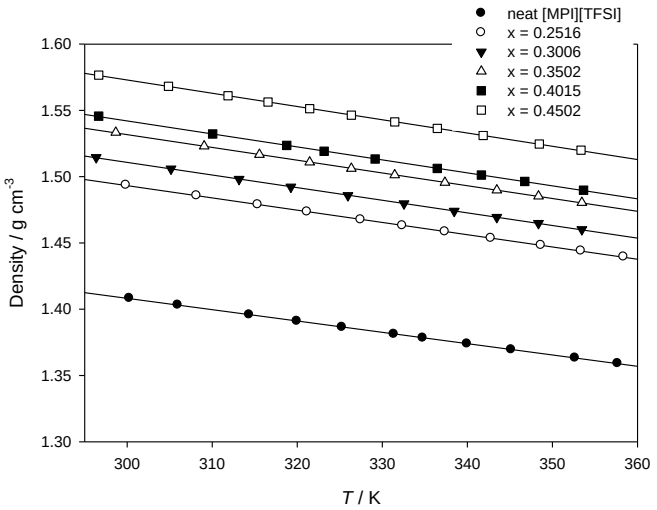

Figure 1. Temperature dependence of density data for neat [MPI][TFSI] and LiTFSI-doped [MPI][TFSI].

Knowledge of electrolyte solutions viscosity is needed for the design of numerous processes and, at the same time, provides useful insights into solution structure and interactions [50]. The relative viscosity (Li-salt-doped sample/neat RTIL sample) is depicted in Fig. 2. The viscosity values, η, were fitted using Vogel–Tamman–Fulcher (VTF) equation and modified Vogel–Tamman–Fulcher (modified VTF) equation [51-52]. The most commonly used equation to correlate the variation of viscosity with temperature is the Arrhenius-like law, but according to Seddon et al. [53], the Arrhenius

law can generally be applied when the cation presents only a limited symmetry. If this is not the case, Vogel–Tamman–Fulcher (VTF) and modified equation Vogel–Tamman–Fulcher are recommended [53]. The modified VTF equation can be expressed as:

$$\eta^{-1} = \frac{\eta_o}{\sqrt{T}} \exp[\frac{-B}{(T - T_o)}] \quad (3)$$

and the VTF equation can be presented as:

$$\eta^{-1} = \eta_o \exp[\frac{-B}{(T - T_o)}] \quad (4)$$

where η_o, B, and T_o are adjustable parameters. The best-fit η_o (mPa s), B (K), and T_o (K) parameters are given in Table 2. The viscosity of neat [MPI][TFSI] and LiTFSI-doped [MPI][TFSI] follows the order: neat [MPI][TFSI] < (x_{LiTFSI} is 0.2516) < (x_{LiTFSI} is 0.3006) < (x_{LiTFSI} is 0.3502) < (x_{LiTFSI} is 0.4015) < (x_{LiTFSI} is 0.4502). The addition of a Li salt to [MPI][TFSI] increased viscosity due to the enhancement of ion-ion interactions.

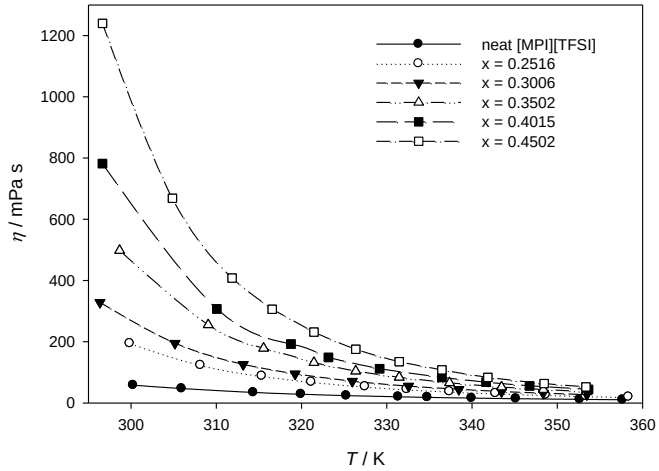

Figure 2. Dynamic viscosity (η) as a function of temperature for neat [MPI][TFSI] and LiTFSI-doped [MPI][TFSI].

For the relationship of η vs. T, the E_a, ΔS, and ΔH values evaluated using the slope ($-E_a/R$) of the Arrhenius equation and Eyring equation for the ILs are summarized in Table 3. The absolute values of E_a, ΔS, and ΔH for the ILs are in the order: (1) LiTFSI-doped [MPI][TFSI], x_{LiTFSI} = 0.2516 (E_a = 34.18 kJ mole^{-1}, $|\Delta S|$ = 324.92 J mole^{-1} K^{-1}, and ΔH = 36.91 kJ mole^{-1}) > [MPI][TFSI] without doping LiTFSI (E_a = 26.59 kJ mole^{-1}, $|\Delta S|$ = 309.92 J mole^{-1} K^{-1}, and ΔH = 29.59 kJ mole^{-1}); (2) higher mole fraction of LiTFSI (x_{LiTFSI} : 0.3502, E_a = 41.15 kJ mole^{-1}, $|\Delta S|$ = 340.95 J mole^{-1} K^{-1}, and ΔH = 43.85 kJ mole^{-1}) > lower mole fraction of LiTFSI (x_{LiTFSI} : 0.3006, E_a = 37.53 kJ mole^{-1}, $|\Delta S|$ = 333.15 J mole^{-1} K^{-1}, and ΔH = 40.22 kJ mole^{-1}).

Table 2. The VTF equation parameters of viscosity ($\eta = \eta_o \exp[B/(T - T_o)]$) and conductivity ($\sigma = \sigma_o \exp[-B'/(T - T_o)]$).

Mole fraction of LiTFSI	η				σ			
	η_o / mPa s	T_o / K	B / K	R^{2a}	σ_o / mS cm^{-1}	T_o / K	B' /K	R^{2a}
neat [MPI][TFSI]	0.191	164.0	780.3	0.999	21.1	214.9	163.1	0.999
x_{LiTFSI} = 0.2516	0.237	184.1	777.0	0.999	35.7	201.6	341.4	0.999
x_{LiTFSI} = 0.3006	0.153	177.6	911.7	0.999	14.7	239.5	168.7	0.999
x_{LiTFSI} = 0.3502	0.151	182.6	939.8	0.999	17.8	231.9	228.0	0.999
x_{LiTFSI} = 0.4015	0.265	194.8	814.2	0.999	18.9	234.3	250.2	0.999
x_{LiTFSI} = 0.4502	0.136	187.1	998.6	0.999	19.5	232.4	291.5	0.999

[a] Correlation coefficient.

Table 3. The E_a, ΔS and ΔH evaluated by Eyring equation and the relationships of η vs. T and σ vs. T.

Mole fraction of LiTFSI	η			σ		
	E_a/ kJ mole^{-1}	ΔS/ J mole^{-1} K^{-1}	ΔH/ kJ mole^{-1}	E_a/ kJ mole^{-1}	ΔS/ J mole^{-1} K^{-1}	ΔH/ kJ mole^{-1}
neat [MPI][TFSI]	26.59	-309.92	29.59	13.28	-199.89	10.65
x_{LiTFSI} = 0.2516	34.18	-324.92	36.91	19.32	-188.28	16.58
x_{LiTFSI} = 0.3006	37.53	-333.15	40.22	22.17	-180.41	19.48
x_{LiTFSI} = 0.3502	41.15	-340.95	43.85	23.96	-177.50	21.24
x_{LiTFSI} = 0.4015	43.46	-346.13	46.16	28.84	-164.43	26.16
x_{LiTFSI} = 0.4502	48.20	-358.16	50.90	32.15	-157.28	29.46

The conductivity of ionic liquids is inversely linked to their viscosity. Hence, ionic liquids with higher viscosity exhibit lower conductivity. The temperature dependence of conductivity for these Li-doped ILs is depicted in Fig. 3. An increase in temperature results in an increase in the mobility because the viscosity of the liquids is reduced. The observed temperature dependences of conductivity are well fitted by VTF equation:

$$\sigma = \sigma_o \exp[\frac{-B'}{(T - T_o)}] \quad (5)$$

where σ_o, B', and T_o were the fitting parameters. The VTF fitting parameters of the ionic conductivity for these ILs are summarized in Table 2. Different from viscosity, the conductivity of ILs decreases with increasing concentration of LiTFSI following the order: neat [MPI][TFSI] > (x_{LiTFSI} is 0.2516) > (x_{LiTFSI} is 0.3006) > (x_{LiTFSI} is 0.3502) > (x_{LiTFSI} is 0.4015) > (x_{LiTFSI} is 0.4502). For the relationship of σ vs. T, the E_a, ΔS, and ΔH values evaluated using the slope ($-E_a$/R) of the Arrhenius

and Eyring equations for the ILs are summarized in Table 3, E_a, ΔS, and ΔH increases with increasing concentration of LiTFSI.

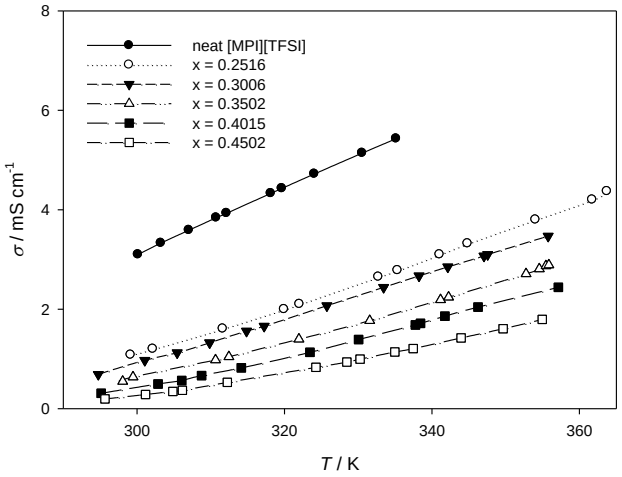

Figure 3. Dependence of specific conductivity (σ) on temperature for neat [MPI][TFSI] and LiTFSI-doped [MPI][TFSI].

The molar conductivity Λ (S cm^2 mol^{-1}) was obtained by dividing the ionic conductivity by the salt concentration according to the following equation:

$$\Lambda = \sigma \frac{M}{\rho} \qquad (6)$$

where M, σ, ρ are the respective equivalent weight, specific conductivity, and density of the IL mixtures. The temperature dependence of molar conductivity for the IL mixtures is depicted in Figure 4. The observed temperature dependences of molar conductivity are well fitted by the empirical VTF equation:

$$\Lambda = \Lambda_o \exp[\frac{-B'}{(T - T_o)}] \qquad (7)$$

where Λ_o, B', and T_o are the fitting parameters. VTF fitting parameters of the molar conductivity for the ILs are summarized in Table 4. With regard to the relationship of Λ vs. T, the E_a, ΔS, and ΔH values evaluated using the slope ($-E_a$/R) of the Arrhenius and Eyring equations for the ILs are summarized in Table 5. The E_a, ΔS, and ΔH values of the molar conductivity (Λ) show similar tendency with specific conductivity (σ).

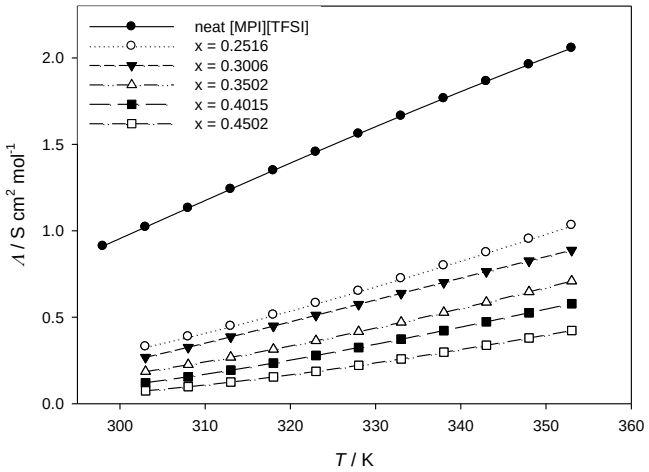

Figure 4. Dependence of molar conductivity (Λ) on temperature for neat [MPI][TFSI] and LiTFSI-doped [MPI][TFSI].

Table 4. VTF equation parameters of molar conductivity data ($\Lambda = \Lambda_o \exp[-B'/(T - T_o)]$, $\Lambda_{NMR} = \Lambda_o \exp[-B'/(T - T_o)]$)

Molar fraction of LiTFSI	Λ				Λ_{NMR}			
	Λ_o / S cm^2 mol^{-1}	T_o/K	B' /K	R^{2a}	Λ_o / S cm^2 mol^{-1}	T_o /K	B' /K	R^{2a}
neat [MPI][TFSI]	7.5	210.6	184.1	0.999	110.4	215.9	362.4	0.999
x_{LiTFSI} = 0.2516	11.2	198.3	369.4	0.999	213.7	197.1	618.5	0.999
x_{LiTFSI} = 0.3006	4.3	237.3	181.9	0.999	276.5	195.8	704.5	0.999
x_{LiTFSI} = 0.3502	9.6	205.9	382.6	0.999	187.7	204.1	658.8	0.999
x_{LiTFSI} = 0.4015	5.2	232.6	264.8	0.999	120.6	212.7	577.8	0.999
x_{LiTFSI} = 0.4502	5.2	230.7	306.7	0.999	102.5	218.1	576.6	0.999

[a] Correlation coefficient.

The Walden plot was used to appreciate the ionicity in ionic liquids. If the viscosity and conductivity of the electrolyte obeys Walden's rule, the ionic conductivity is correlated to viscosity using the qualitative approach of Angell et al. [54]:

$$\Lambda \eta^{\alpha} = C \qquad (8)$$

where C is a temperature-dependent constant, which is called the Walden product. α is the slope of the line in the Walden plot, which reflects the decoupling of the ions. The fitted α values of

the ILs are given in Table 6. The parameter α reflects the difference of the activation energies of the ionic conductivity and viscosity. In the present study, all α values are smaller than unity ($\alpha < 1$), indicating that the ionic conductivities of the liquid salts is somewhat diminished as a result of ion-pair formation [55]. Moreover, combining the data from viscosity, conductivity and density measurements we find the molar conductivities of ILs with x_{LiTFSI} = 0, 0.2516, 0.3006, 0.3502, 0.4015, and 0.4502 to be 1.021, 0.330, 0.268, 0.186, 0.121, and 0.075 S cm^2 mol^{-1} at 30 ^{o}C, respectively. Another method that yields almost identical values of α is the ratio of the temperature-dependent activation energies for viscosity and molar conductivity, $E_{a,\Lambda}/E_{a,\eta}$. The activation energies of $E_{a,\Lambda}$ and $E_{a,\eta}$ are summarized in Table 3 and Table 5. Table 6 compares α values calculated from the slopes of the Walden plots in Fig. 5 with those calculated from the activation energies. The two methods for obtaining α values are in very good agreement.

According to the Walden rule, ILs that possess strongly interacting ions in ILs are usually located below the KCl ideal line, due to partial association of neighboring ions. In the present study, LiTFSI-doped [MPI][TFSI] and neat [MPI][TFSI] are less than the $\Lambda\eta$ of the KCl aqueous solution, indicating a fraction of ion association in the ILs. Compare the discrepancy from the ideal line of Walden plots, the deviation increases significantly with the addition of LiTFSI to [MPI][TFSI], implying the addition of LiTFSI increases the ion association in the IL mixture.

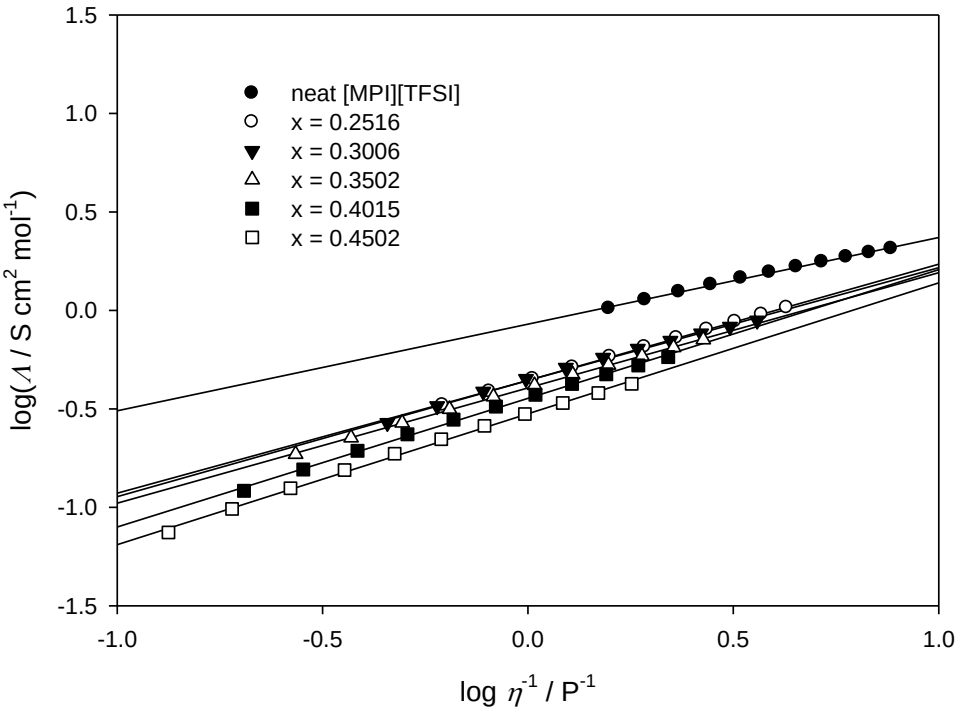

Figure 5. Walden plots for neat [MPI][TFSI] and LiTFSI-doped [MPI][TFSI], where Λ is the equivalent conductivity and η^{-1} is the fluidity. The solid lines are the result of linear regressions onto the data.

Table 5. The E_a, ΔS and ΔH evaluated by Eyring equation and the relationships of Λ vs. T and Λ_{NMR} vs. T.

Molar fraction of LiTFSI	Λ			Λ_{NMR}		
	E_a/ kJ mole^{-1}	ΔS/ J mole^{-1} K^{-1}	ΔH/ kJ mole^{-1}	E_a/ kJ mole^{-1}	ΔS/ J mole^{-1} K^{-1}	ΔH/ kJ mole^{-1}
neat [MPI][TFSI]	12.79	-211.40	10.10	26.69	-160.74	23.98
x_{LiTFSI} = 0.2516	20.14	-196.38	17.42	32.94	-148.64	30.22
x_{LiTFSI} = 0.3006	20.93	-195.17	18.21	36.63	-140.27	33.91
x_{LiTFSI} = 0.3502	23.64	-189.50	20.92	39.48	-134.78	36.77
x_{LiTFSI} = 0.4015	27.39	-180.30	24.68	40.39	-133.20	37.67
x_{LiTFSI} = 0.4502	30.46	-174.17	27.74	44.74	-123.30	42.02

Table 6. Comparison of the activation energies for the absolute viscosity, $E_{a,\eta}$, and equivalent conductance, $E_{a,\Lambda}$. α is from the general Walden plots and α_{EA} is calculated from the ratio of the activation energies ($E_{a,\Lambda}$ / $E_{a,\eta}$).

Molar fraction of LiTFSI	$E_{a,\eta}$ / kJ mole^{-1}	$E_{a,\Lambda}$ / kJ mole^{-1}	α	α_{EA}
neat [MPI][TFSI]	26.59	12.79	0.44	0.48
x_{LiTFSI} = 0.2516	34.18	20.14	0.59	0.59
x_{LiTFSI} = 0.3006	37.53	20.93	0.57	0.56
x_{LiTFSI} = 0.3502	41.15	23.64	0.58	0.57
x_{LiTFSI} = 0.4015	43.46	27.39	0.65	0.63
x_{LiTFSI} = 0.4502	48.20	30.46	0.66	0.63

3.2. Self-Diffusion Coefficient of the Individual ion

One of the most powerful methods to study molecular motion is the pulsed-gradient spin-echo (PGSE) NMR technique, which were carried out to determine the self-diffusion coefficients of individual ion in neat [MPI][TFSI] and LiTFSI-doped [MPI][TFSI]. The diffusion coefficients of the ^{1}H, ^{7}Li, and ^{19}F nuclei have been measured as a function of the LiTFSI mole fraction in [MPI][TFSI] and LiTFSI mixtures for $0 < x_{LiTFSI} < 0.45$. For consistency of self-diffusion coefficient determination, the hydrogen adjacent to the two nitrogen atoms in imidazolium was selected in this study. Fig. 6 shows the temperature dependence of the self-diffusion coefficients of the cation and anion species (D_{MPI^+}, D_{Li^+}, and D_{TFSI^-}), and the summation of the cation and anion ($D_{total} = x D_{Li^+} + (1-x) D_{MPI^+} + D_{TFSI^-}$) for these binary IL solutions, the experimental self-diffusion coefficients D (cm^2 s^{-1}) for LiTFSI-doped [MPI][TFSI] and neat [MPI][TFSI] are summarized in Table 7. As shown in Fig. 6, some of the temperature dependence curves of D_{MPI^+}, D_{Li^+}, D_{TFSI^-}, and D_{total} cannot be expressed by a simple linear function. However, the Vogel–Tamman–Fulcher (VTF) equation fits the experimental data very well over the entire temperature range.

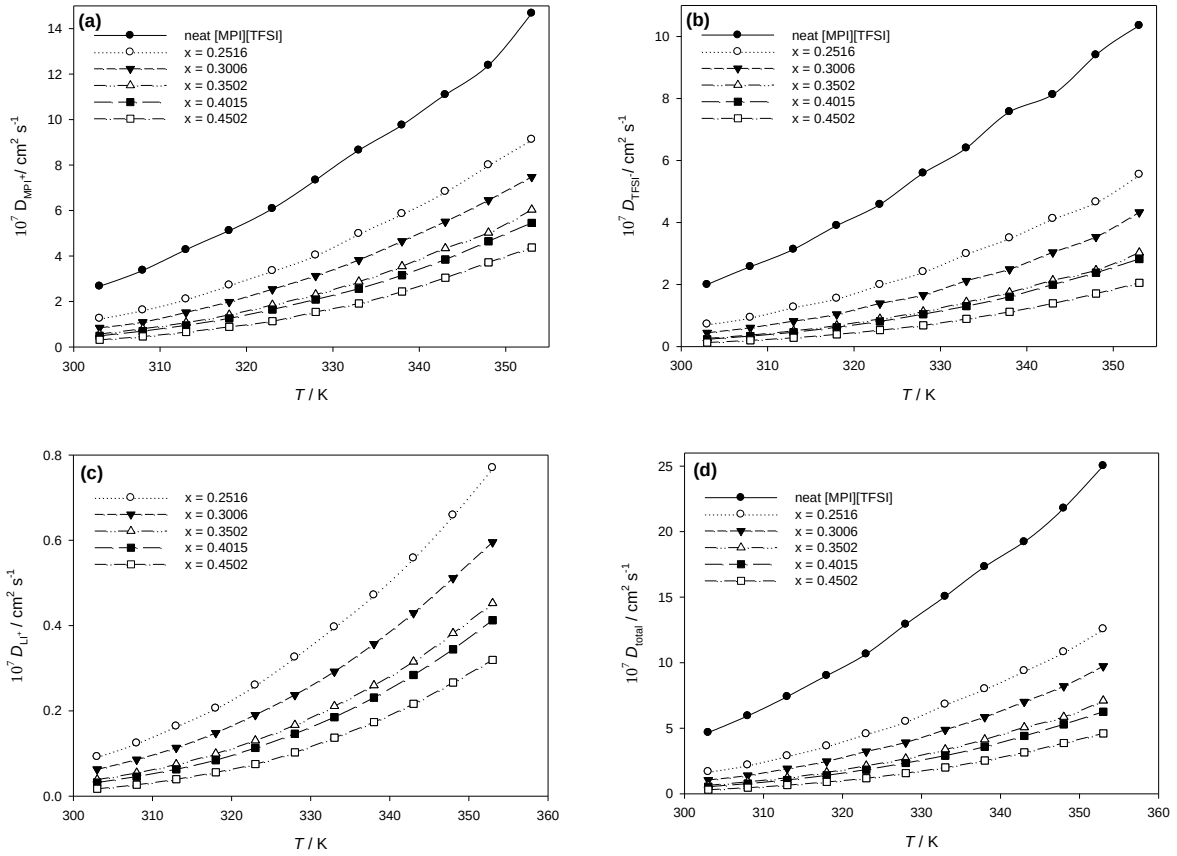

Figure 6. Temperature dependence of the self-diffusion coefficients of ions (a) D_{MPI^+}, (b) D_{TFSI^-}, (c) D_{Li^+}, and (d) D_{total} in neat [MPI][TFSI] and LiTFSI-doped [MPI][TFSI].

$$D = D_{\mathrm{o}} \exp[\frac{-B'}{(T - T_{\mathrm{o}})}] \qquad (9)$$

where the constants D_{o} (cm^2 s^{-1}), B (K), and T_{o} (K) are adjustable parameters. The best-fit parameters of the ionic diffusivity are summarized in Table 8 and Table 9. For the relationship of D vs. T, the E_{a}, ΔS, and ΔH values evaluated using the slope ($-E_{\mathrm{a}}$/R) of the Arrhenius and Eyring equations for the ILs are summarized in Table 10 and Table 11. As shown in Fig. 6, the sum of the cationic and anionic diffusion coefficients (D_{total}) for the neat [MPI][TFSI] and LiTFSI-doped [MPI][TFSI] follows the order: ($x_{\mathrm{LiTFSI}} = 0$) > ($x_{\mathrm{LiTFSI}} = 0.2516$) > ($x_{\mathrm{LiTFSI}} = 0.3006$) > ($x_{\mathrm{LiTFSI}} = 0.3502$) > ($x_{\mathrm{LiTFSI}} = 0.4015$) > ($x_{\mathrm{LiTFSI}} = 0.4502$).

Ionic transference numbers at 303 K are shown in Table 7 to compare the self-diffusion coefficients of each ion, the ionic transference number t_{i} [56] is defined as:

$$t_{\mathrm{i}} = \frac{x_{\mathrm{i}} D_{\mathrm{i}}}{\Sigma x_{\mathrm{i}} D_{\mathrm{i}}} \qquad (10)$$

The ionic transference numbers of ions in ILs can be ascribed to influence by the shape of the ions and the local interaction between the cations and anions [57]. As shown in Table 7, the ionic transference number of the MPI^+ is larger than that of $TFSI^-$ in neat [MPI][TFSI] and LiTFSI-doped [MPI][TFSI], and the ionic transference numbers of the Li^+ increase with increasing LiTFSI mole fraction in [MPI][TFSI] and LiTFSI mixtures.

3.3. Molar conductivity evaluated from the PGSE-NMR diffusion coefficients

The Nernst-Einstein equation is applied to calculate molar conductivity (Λ_{NMR}) from the PGSE-NMR diffusion coefficients:

$$\Lambda_{NMR} = \frac{Ne^2(x_{MPI^+}D_{MPI^+} + D_{TFSI^-} + x_{Li^+}D_{Li^+})}{kT} \qquad (11)$$

where N is the Avogadro number, e is the electric charge on each ionic carrier ($1.602*10^{-19}$ Coulomb), x_{MPI^+} and x_{Li^+} are the molar ratio of IL and LiTFSI, respectively, k is the Boltzmann constant ($1.38*10^{-23}$), and T is the absolute temperature (K). The temperature dependence of the molar conductivity calculated from the ionic diffusion coefficient and Eq. 11 is shown in Fig. 7 and the best-fit parameters of the VTF equation are listed in Table 4. The experimental molar conductivity value (Λ) is lower than that of the calculated molar conductivity (Λ_{NMR}) over the entire temperature range, implying ion association in ionic liquids [58].

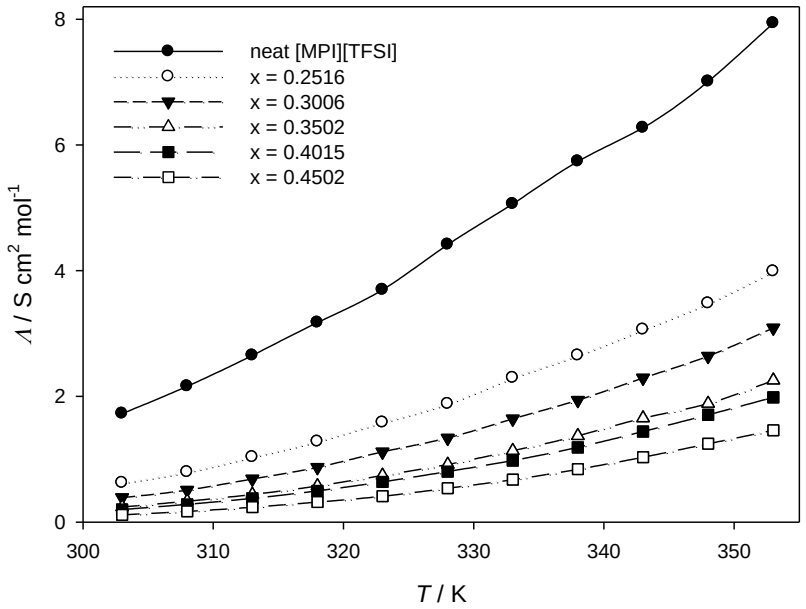

Figure 7. Dependence of molar conductivity (Λ_{NMR}) on temperature for neat [MPI][TFSI] and LiTFSI-doped [MPI][TFSI]. Λ_{NMR} is calculated from PGSE-NMR diffusion coefficient and Nernst-Einstein equation.

Table 7. Experimental self-diffusion coefficients D (cm^2 s^{-1}) and ion transference number t at 303 K for LiTFSI-doped [MPI][TFSI] and neat [MPI][TFSI]. Transference number t_i is defined as: $t_i = x_iD_i/\Sigma x_iD_i$.

	ion	D / cm^2 s^{-1}	t
neat [MPI][TFSI]	MPI^+	2.67×10^{-7}	0.572
	$TFSI^-$	2.00×10^{-7}	0.428
x_{LiTFSI} = 0.2516	MPI^+	1.26×10^{-7}	0.558
	Li^+	9.25×10^{-9}	0.014
	$TFSI^-$	7.22×10^{-8}	0.429
x_{LiTFSI} = 0.3006	MPI^+	8.45×10^{-8}	0.560
	Li^+	6.28×10^{-9}	0.018
	$TFSI^-$	4.46×10^{-8}	0.422
x_{LiTFSI} = 0.3502	MPI^+	5.69×10^{-8}	0.571
	Li^+	3.88×10^{-9}	0.021
	$TFSI^-$	2.65×10^{-8}	0.409
x_{LiTFSI} = 0.4015	MPI^+	4.91×10^{-8}	0.543
	Li^+	3.20×10^{-9}	0.024
	$TFSI^-$	2.35×10^{-8}	0.434
x_{LiTFSI} = 0.4502	MPI^+	3.15×10^{-8}	0.557
	Li^+	1.73×10^{-9}	0.025
	$TFSI^-$	1.30×10^{-8}	0.418

Table 8. VTF equation parameters of self-diffusion coefficient data ($D = D_o \exp[-B'/(T - T_0)]$) from the MPI^+ of [MPI][TFSI] and $TFSI^-$ of LiTFSI and [MPI][TFSI].

Molar fraction of LiTFSI	D_{MPI}^+				D_{TFSI}-			
	D_o/cm^2 s^{-1}	T_o (K)	B' (K)	R^{2a}	D_o/cm^2 s^{-1}	T_o (K)	B' (K)	R^{2a}
neat [MPI][TFSI]	3.94×10^{-5}	203.8	495.4	0.999	2.12×10^{-5}	212.4	422.5	0.999
x_{LiTFSI} = 0.2516	1.12×10^{-4}	183.9	809.2	0.999	4.83×10^{-5}	194.0	709.8	0.999
x_{LiTFSI} = 0.3006	1.76×10^{-4}	182.1	924.7	0.999	5.51×10^{-5}	194.6	771.6	0.999
x_{LiTFSI} = 0.3502	7.52×10^{-5}	200.1	739.7	0.999	5.58×10^{-5}	196.1	818.5	0.999
x_{LiTFSI} = 0.4015	4.60×10^{-5}	209.8	637.9	0.999	3.36×10^{-5}	206.2	702.9	0.999
x_{LiTFSI} = 0.4502	7.01×10^{-5}	205.6	750.5	0.999	1.44×10^{-5}	223.5	556.9	0.999

[a] Correlation coefficient.

Table 9. VTF equation parameters of self-diffusion coefficient data ($D = D_o \exp[-B'/(T - T_o)]$) from Li^+ of LiTFSI and ($MPI^+ + TFSI^- + Li^+$) of (LiTFSI and [MPI][TFSI]).

Molar fraction of LiTFSI	D_{Li}^+				D_{total}			
	D_o/cm^2 s^{-1}	T_o (K)	B' (K)	R^{2a}	D_o/cm^2 s^{-1}	T_o (K)	B' (K)	R^{2a}
neat [MPI][TFSI]	---	---	---	---	5.96×10^{-5}	207.6	462.6	0.999
$x_{LiTFSI} = 0.2516$	7.85×10^{-6}	193.3	739.4	0.999	1.31×10^{-4}	188.7	761.8	0.999
$x_{LiTFSI} = 0.3006$	1.09×10^{-5}	187.8	859.4	0.999	1.75×10^{-4}	187.6	856.0	0.999
$x_{LiTFSI} = 0.3502$	1.10×10^{-5}	191.7	884.0	0.999	1.05×10^{-4}	198.3	774.3	0.999
$x_{LiTFSI} = 0.4015$	1.23×10^{-5}	191.6	919.9	0.999	6.33×10^{-5}	207.7	673.1	0.999
$x_{LiTFSI} = 0.4502$	5.96×10^{-6}	213.7	727.4	0.999	5.08×10^{-5}	214.1	657.2	0.999

[a] Correlation coefficient.

Table 10. The E_a, ΔS and ΔH evaluated by Eyring equation and the relationships of D_{MPI}^+ vs. T and D_{TFSI}- vs. T.

Molar fraction of LiTFSI	D_{MPI}^+			D_{TFSI}-		
	E_a/ kJ mole^{-1}	ΔS/ J mole^{-1} K^{-1}	ΔH/ kJ mole^{-1}	E_a/ kJ mole^{-1}	ΔS/ J mole^{-1} K^{-1}	ΔH/ kJ mole^{-1}
neat [MPI][TFSI]	29.61	-281.55	26.89	29.13	-285.42	26.42
$x_{LiTFSI} = 0.2516$	35.34	-268.94	32.62	36.00	-271.28	33.28
$x_{LiTFSI} = 0.3006$	38.98	-260.15	36.26	39.80	-262.70	37.08
$x_{LiTFSI} = 0.3502$	41.61	-254.58	38.90	42.92	-256.60	40.20
$x_{LiTFSI} = 0.4015$	42.37	-253.22	39.65	43.87	-254.41	41.15
$x_{LiTFSI} = 0.4502$	46.54	-243.13	43.82	48.32	-244.30	45.61

Table 11. The E_a, ΔS and ΔH evaluated by Eyring equation and the relationships of D_{Li}^+ vs. T and D_{total} vs. T.

Molar fraction of LiTFSI	D_{Li}^+			D_{total}		
	E_a/ kJ mole^{-1}	ΔS/ J mole^{-1} K^{-1}	ΔH/ kJ mole^{-1}	E_a/ kJ mole^{-1}	ΔS/ J mole^{-1} K^{-1}	ΔH/ kJ mole^{-1}
neat [MPI][TFSI]	---	---	---	29.41	-277.52	26.69
$x_{LiTFSI} = 0.2516$	33.99	-272.45	31.27	35.65	-265.42	32.94
$x_{LiTFSI} = 0.3006$	37.38	-283.78	34.67	39.35	-257.05	36.63
$x_{LiTFSI} = 0.3502$	39.90	-278.71	37.18	42.20	-251.56	39.48
$x_{LiTFSI} = 0.4015$	43.50	-270.72	40.78	43.10	-249.98	40.39
$x_{LiTFSI} = 0.4502$	45.25	-266.52	42.53	47.46	-240.08	44.74

3.4. Comparison of the dynamic properties depending on temperature

Fig. 8 shows the activation energies of the reciprocal of viscosity ($1/\eta$), the ionic conductivity (σ), molar conductivity (Λ), and individual ion diffusion coefficients (D_{MPI^+}, D_{Li^+}, and D_{TFSI^-}) against the LiTFSI concentration. The activation energies for the $1/\eta$ are larger than those of the σ and Λ, however, they are comparable to those of individual ion diffusion at $0 < x_{LiTFSI} < 0.45$. The activation energy of $1/\eta$, σ, Λ, D_{MPI^+}, D_{Li^+}, and D_{TFSI^-} showed an increased tendency with increasing LiTFSI concentration, demonstrating a reduction of the translational motions due to the higher viscosity in the concentrated samples. The different tendency between the activation energy of the σ and individual ion diffusion against the LiTFSI concentration can be attributed to different types between σ and individual ion diffusion. The σ is affected by ion transfer velocity and the number of "electrochemically" active ions, but individual ion diffusion coefficients consider the isolated, paired, and clustered ions including non-charge neutral ion clusters.

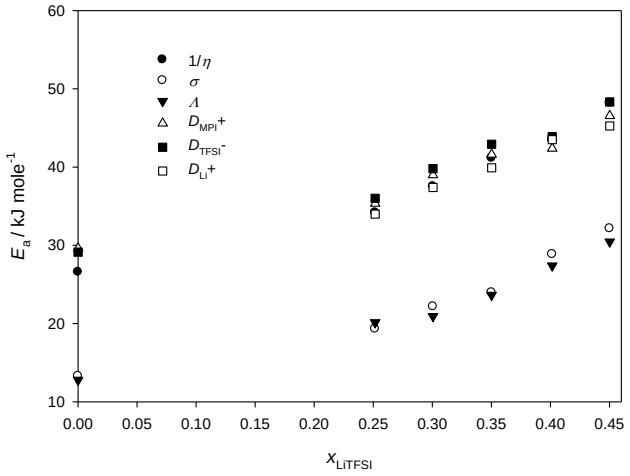

Figure 8. Dependencies of the activation energies of the individual ion diffusion, ionic conductivity, and (reciprocal of the) viscosity in neat [MPI][TFSI] and LiTFSI-doped [MPI][TFSI].

4. CONCLUSIONS

We present a study on the transport properties through conductivity (σ), viscosity (η), and self-diffusion coefficient (D) measurements in [MPI][TFSI]/LiTFSI mixtures with different mole fraction of LiTFSI. Self-diffusion coefficients (D) of the ion species in LiTFSI-doped [MPI][TFSI] systems were determined by observing ^{1}H and ^{19}F nuclei with the pulsed-field gradient spin−echo NMR technique. Results show that the diffusion of each ion depends on the concentration of lithium salt. The comparison between ions' mobility determined by conductivity and by NMR measurements indicates that the conductivity mechanism also depends on the concentration of lithium salt. The density and viscosity in the ILs increased with increasing concentration of LiTFSI, whereas the conductivity, molar conductivity, and self-diffusion coefficient of each ionic species decreased with increasing

concentration of LiTFSI. The correlation between ionic conductivity and viscosity is based on the classical Walden rule, the α values of neat [MPI][TFSI] and LiTFSI-doped [MPI][TFSI] calculated from the slopes of the Walden plots are compared to those calculated from the ratio of activation energies for viscosity and molar conductivity ($E_{a,\Lambda}/E_{a,\eta}$).

ACKNOWLEDGEMENTS
The authors would like to thank the National Science Council of the Republic of China for financially supporting this project.

References

1. R.D. Rogers, K.R. Seddon, Ionic Liquids: Industrial Applications for Green Chemistry, American Chemical Society, Washington, DC, 2003.
2. B. Baek, S. Lee, C. Jung, *Int. J. Electrochem. Sci.*, 6 (2011) 6220.
3. T.Y. Wu, B.K. Chen, L. Hao, K.F. Lin, I.W. Sun, *J. Taiwan Inst. Chem. Eng.*, 42 (2011) 914.
4. N.V. Likhanova, O. Olivares-Xometl, D. Guzman-Lucero, M.A. Dominguez-Aguilar, N. Nava, M. Corrales-Luna, M.C. Mendoza, *Int. J. Electrochem. Sci.*, 6 (2011) 4514.
5. T.Y. Wu, H.C. Wang, S.G. Su, S.T. Gung, M.W. Lin, C.B. Lin, *J. Chin. Chem. Soc.*, 57 (2010) 44.
6. H. Wang, L.X. Wu, Y.C. Lan, J.Q. Zhao, J.X. Lu, *Int. J. Electrochem. Sci.*, 6 (2011) 4218.
7. T.Y. Wu, B.K. Chen, C.W. Kuo, L. Hao, Y.C. Peng, I.W. Sun, *J. Taiwan Inst. Chem. Eng.*, 43 (2012) 860.
8. S.K. Shukla, L.C. Murulana, E.E. Ebenso, *Int. J. Electrochem. Sci.*, 6 (2011) 4286.
9. T.Y. Wu, B.K. Chen, L. Hao, C.W. Kuo, I.W. Sun, *J. Taiwan Inst. Chem. Eng.*, 43 (2012) 313.
10. T.Y. Wu, S.G. Su, S.T. Gung, M.W. Lin, Y.C. Lin, W.C. Ou-Yang, I.W. Sun, C.A. Lai, *J. Iran. Chem. Soc.*, 8 (2011) 149.
11. H.A. Barham, S.A. Brahim, Y. Rozita, K.A. Mohamed, *Int. J. Electrochem. Sci.*, 6 (2011) 181.
12. T.Y. Wu, I.W. Sun, S.T. Gung, B.K. Chen, H.P. Wang, S.G. Su, *J. Taiwan Inst. Chem. Eng.*, 42 (2011) 874.
13. T.Y. Wu, S.G. Su, K.F. Lin, Y.C. Lin, H.P. Wang, M.W. Lin, S.T. Gung, I.W. Sun, *Electrochim. Acta*, 56 (2011) 7278.
14. P.N. Tshibangu, S.N. Ndwandwe, E.D. Dikio, *Int. J. Electrochem. Sci.*, 6 (2011) 2201.
15. T.Y. Wu, S.G. Su, H.P. Wang, I.W. Sun, *Electrochem. Commun.*, 13 (2011) 237.
16. T.Y. Wu, S.G. Su, S.T. Gung, M.W. Lin, Y.C. Lin, C.A. Lai, I.W. Sun, *Electrochim. Acta*, 55 (2010) 4475.
17. L.C. Xuan, Y.X. An, W. Fang, L.X. Liao, Y.L. Ma, Z.Y. Ren, G.P. Yin, *Int. J. Electrochem. Sci.*, 6 (2011) 6590.
18. Y.X. An, P.J. Zuo, X.Q. Cheng, L.X. Liao, G.P. Yin, *Int. J. Electrochem. Sci.*, 6 (2011) 2398.
19. T.Y. Wu, L. Hao, C.W. Kuo, Y.C. Lin, S.G. Su, P.L. Kuo, I.W. Sun, *Int. J. Electrochem. Sci.*, 7 (2012) 2047.
20. S. Ibrahim, M.R. Johan, *Int. J. Electrochem. Sci.*, 6 (2011) 5565.
21. H. Ganjali, M.R. Ganjali, T. Alizadeh, F. Faridbod, P. Norouzi, *Int. J. Electrochem. Sci.*, 6 (2011) 6085.
22. M.R. Ganjali, H. Ganjali, M. Hosseini, P. Norouzi, *Int. J. Electrochem. Sci.*, 5 (2010) 967.
23. M.R. Ganjali, S. Aghabalazadeh, M. Rezapour, M. Hosseini, P. Norouzi, *Int. J. Electrochem. Sci.*, 5 (2010) 1743.
24. M. Pandurangachar, B.E.K. Swamy, B.N. Chandrashekar, O. Gilbert, S. Reddy, B.S. Sherigara, *Int. J. Electrochem. Sci.*, 5 (2010) 1187.

25. P. Norouzi, Z. Rafiei-Sarmazdeh, F. Faridbod, M. Adibi, M.R. Ganjali, *Int. J. Electrochem. Sci.*, 5 (2010) 367.
26. F. Faridbod, M.R. Ganjali, M. Pirali-Hamedani, P. Norouzi, *Int. J. Electrochem. Sci.*, 5 (2010) 1103.
27. M.R. Ganjali, M.H. Eshraghi, S. Ghadimi, S.M. Moosavi, M. Hosseini, H. Haji-Hashemi, P. Norouzi, *Int. J. Electrochem. Sci.*, 6 (2011) 739.
28. M.R. Ganjali, T. Poursaberi, M. Khoobi, A. Shafiee, M. Adibi, M. Pirali-Hamedani, P. Norouzi, *Int. J. Electrochem. Sci.*, 6 (2011) 717.
29. P. Norouzi, M. Hosseini, M.R. Ganjali, M. Rezapour, M. Adibi, *Int. J. Electrochem. Sci.*, 6 (2011) 2012.
30. M.R. Ganjali, M.R. Moghaddam, M. Hosseini, P. Norouzi, *Int. J. Electrochem. Sci.*, 6 (2011) 1981.
31. M.R. Ganjali, M. Hosseini, M. Pirali-Hamedani, H.A. Zamani, *Int. J. Electrochem. Sci.*, 6 (2011) 2808.
32. M.R. Ganjali, M. Rezapour, S.K. Torkestani, H. Rashedi, P. Norouzi, *Int. J. Electrochem. Sci.*, 6 (2011) 2323.
33. P. Norouzi, M. Pirali-Hamedani, S.O. Ranaei-Siadat, M.R. Ganjali, *Int. J. Electrochem. Sci.*, 6 (2011) 3704.
34. F. Faridbod, H.A. Zamani, M. Hosseini, M. Pirali-Hamedani, M.R. Ganjali, P. Norouzi, *Int. J. Electrochem. Sci.*, 6 (2011) 3694.
35. M.R. Ganjali, S.O. Ranaei-Siadat, H. Rashedi, M. Rezapour, P. Norouzi, *Int. J. Electrochem. Sci.*, 6 (2011) 3684.
36. T.H. Tsai, K.C. Lin, S.M. Chen, *Int. J. Electrochem. Sci.*, 6 (2011) 2672.
37. M.R. Ganjali, T. Alizadeh, F. Azimi, B. Larjani, F. Faridbod, P. Norouzi, *Int. J. Electrochem. Sci.*, 6 (2011) 5200.
38. T.Y. Wu, M.H. Tsao, F.L. Chen, S.G. Su, C.W. Chang, H.P. Wang, Y.C. Lin, W.C. Ou-Yang, I.W. Sun, *Int. J. Mol. Sci.*, 11 (2010) 329.
39. S.Y. Ku, S.Y. Lu, *Int. J. Electrochem. Sci.*, 6 (2011) 5219.
40. T.Y. Wu, M.H. Tsao, F.L. Chen, S.G. Su, C.W. Chang, H.P. Wang, Y.C. Lin, I.W. Sun, *J. Iran. Chem. Soc.*, 7 (2010) 707.
41. M.H. Tsao, T.Y. Wu, H.P. Wang, I.W. Sun, S.G. Su, Y.C. Lin, C.W. Chang, *Mater. Lett.*, 65 (2011) 583.
42. T.Y. Wu, M.H. Tsao, S.G. Su, H.P. Wang, Y.C. Lin, F.L. Chen, C.W. Chang, I.W. Sun, *J. Braz. Chem. Soc.*, 22 (2011) 780.
43. I.W. Sun, H.P. Wang, H. Teng, S.G. Su, Y.C. Lin, C.W. Kuo, P.R. Chen, T.Y. Wu, *Int. J. Electrochem. Sci.*, 7 (2012) 9748.
44. J. Gao, J.G. Liu, W.M. Liu, B. Li, Y.C. Xin, Y. Yin, Z.G. Zou, *Int. J. Electrochem. Sci.*, 6 (2011) 6115.
45. T.Y. Wu, S.G. Su, Y.C. Lin, H.P. Wang, M.W. Lin, S.T. Gung, I.W. Sun, *Electrochim. Acta*, 56 (2010) 853.
46. I.W. Sun, Y.C. Lin, B.K. Chen, C.W. Kuo, C.C. Chen, S.G. Su, P.R. Chen, T.Y. Wu, *Int. J. Electrochem. Sci.*, 7 (2012) 7206.
47. T.Y. Wu, B.K. Chen, L. Hao, Y.C. Peng, I.W. Sun, *Int. J. Mol. Sci.*, 12 (2011) 2598.
48. T.Y. Wu, H.C. Wang, S.G. Su, S.T. Gung, M.W. Lin, C.B. Lin, *J. Taiwan Inst. Chem. Eng.*, 41 (2010) 315.
49. J.E. Tanner, E.O. Stejskal, *J. Chem. Phys.*, 49 (1968) 1768.
50. T.Y. Wu, I.W. Sun, S.T. Gung, M.W. Lin, B.K. Chen, H.P. Wang, S.G. Su, *J. Taiwan Inst. Chem. Eng.*, 42 (2011) 513.
51. T.Y. Wu, S.G. Su, H.P. Wang, Y.C. Lin, S.T. Gung, M.W. Lin, I.W. Sun, *Electrochim. Acta*, 56 (2011) 3209.

52. T.Y. Wu, I.W. Sun, M.W. Lin, B.K. Chen, C.W. Kuo, H.P. Wang, Y.Y. Chen, S.G. Su, *J. Taiwan Inst. Chem. Eng.*, 43 (2012) 58.
53. K.R. Seddon, A.S. Starck, M.J. Torres, ACS Symposium Series 901, Washington, DC, 2004.
54. M. Yoshizawa, W. Xu, C.A. Angell, *J. Am. Chem. Soc.*, 125 (2003) 15411.
55. H. Ohno, Electrochemical Aspects of Ionic Liquids, Wiley, New Jersey, 2005.
56. F. Castiglione, E. Ragg, A. Mele, G.B. Appectecchi, M. Montanino, S. Passerini, *J. Phys. Chem. Lett*., 2 (2011) 153.
57. J.-C. Lassegues, J. Grondin, C. Aupetit, P. Johansson, *J. Phys. Chem. A*, 113 (2009) 305.
58. H. Tokuda, K. Hayamizu, K. Ishii, M.A.B.H. Susan, M. Watanabe, *J. Phys. Chem. B*, 109 (2005) 6103.